IMPROVED SUBAPERTURE BASED APERTURE-DEPENDENT MOTION COMPENSATION BASED ON ADAPTIVE BLOCKING AND APODIZATION

Rifat Afroz*, Rolf Scheiber†, Brian Ng*, Derek Abbott*

* School of Electrical and Electronic Engineering, The University of Adelaide, Australia

† Microwaves and Radar Institute, German Aerospace Center (DLR), Germany

Email: rifat.afroz@adelaide.edu.au

ABSTRACT

Subaperture Topography and Aperture (SATA) dependent azimuthal motion compensation (MOCO) can yield satisfactory target focusing at slow to moderate track deviations. However, at faster track deviations, the algorithm has to make a trade-off between handling higher motion error frequency and finer instantaneous squint angles. Subaperture selection plays a crucial role in the overall performance of SATA. This paper proposes two techniques based on adaptive blocking and complex dual apodization (CDA) to improve the performance of SATA in the presence of high frequency motion error. The techniques are verified both using simulated and real L-band datasets. A significant improvement in the overall focusing quality of far range targets is achieved using the adaptive technique. The apodization based scheme can improve both the resolution and sidelobe levels that are otherwise traded-off in a fixed block length SATA.

Index Terms— Synthetic Aperture Radar (SAR), motion compensation, subaperture.

1. INTRODUCTION

In wide-beam or squinted SAR systems, aperture-dependent correction in conjunction with two step MOCO is necessary to achieve high resolution [1]. Some well-defined techniques that rely on the time-frequency relationship are available in the literature [1–3]. Among those, SATA is the most computationally efficient that gives sufficient focusing accuracy for slow to moderate track deviations [4]. However, the performance of the algorithm degrades when fast varying motion error is encountered. A smaller block size is preferable for handling such deviations, which on the other hand reduces its capability to provide finer instantaneous squint angle within the subaperture. In such cases, a compromise is made by the algorithm in choosing a fixed block size.

An improvement of the SATA algorithm has been proposed to improve the sidelobe levels in SATA [5]. Although effective, the technique is based on the scaled fourier transform (SFT) that is computationally expensive. As it relies

on fixed block length, the trade-off in original SATA still remains unresolved. The performance improvement of SATA based on its parameter selection is not addressed in the existing literature as to date.

This paper proposes two techniques to circumvent the SATA trade-off problem. The first technique relies on the adaptive selection of subaperture blocks based on the frequency of motion error and range variation within the scene. The second one is based on the concept of complex dual apodization (CDA) [6] that improves the target focusing quality, by performing apodization on two SAR images focused using SATA with different block sizes. Demonstrations of the proposed methods using simulated and real L-band dataset are provided.

2. EFFECTS OF SUBAPERTURE SIZE ON THE PERFORMANCE OF SATA

The subaperture size impacts the focusing qualities of the targets obtained through performing SATA. The algorithm divides the entire synthetic aperture into small blocks and utilizes line-of-sight (LOS) motion error of the mid-block sample to correct aperture-dependent error of the rest of the azimuthal samples within the block. For high frequency motion errors, the blocks need to be small so that the constant motion error assumption within a block still holds. The block length is bounded on the upper and lower ends by [4]

$$\frac{\theta_a}{\theta_{\text{inst}}} \le L \le \frac{\text{PRF}}{2f_{\text{max,me}}},$$
 (1)

where PRF is the pulse repetition frequency and $f_{\rm max,me}$ is the maximum frequency of the aperture dependent motion error and θ_a and $\theta_{\rm inst}$ are the azimuthal beamwidth and instantaneous squint angles, respectively. It implies that L has to be small enough to adequately compensate the maximum frequency component of the motion error. Note that SATA transforms the azimuthal time domain samples in a block into the frequency domain via short-time FFTs and each azimuthal frequency represents a $\theta_{\rm inst}$ of the scene. Equation (1) indicates that if L is made too small, $\theta_{\rm inst}$ becomes coarser. Thus

the aperture dependent error computed for each azimuthal frequency will be very large to accommodate within a given L. Smaller L also decreases the algorithm's computational efficiency.

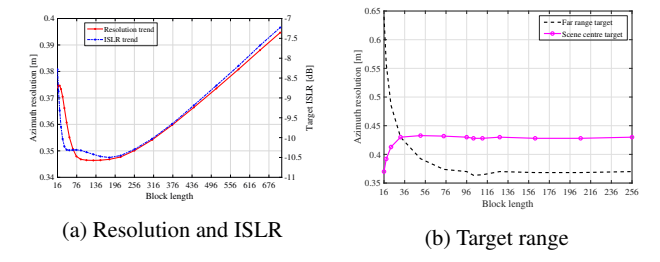


Fig. 1: Effect of block length on target PSF. Stripmap mode is simulated with parameters in Table 1.

Fig. 1a illustrates the impact of SATA block length selection on point spread function (PSF) for a scene centre target using a simulated L-band dataset. The resolution and ISLR are optimal within a block length of 32 and 256, with the performance degrading quickly with increasing block sizes. It shows that for a given motion error frequency, target focusing quality is limited by the choice of block length. Size of blocks can impact differently on targets at different range bin, which is observed in Fig. 1b. The resolution trends indicate that the far range target (at $3.051\,\mathrm{m}$ range) focusing can be improved using larger blocks whereas smaller blocks are preferred for near range targets.

3. TECHNIQUES FOR IMPROVING SATA

3.1. Adaptive blocking

Unlike conventional SATA, the adaptive blocking scheme uses a range of block sizes to improve the motion compensation. It considers both the frequency of motion error and scene range while selecting the length of a subaperture: larger blocks are preferable for providing finer instantaneous squint angle, while smaller blocks are preferred for high frequency motion error. Based on the motion error frequency at each block, the scheme adaptively selects a block size from a preselected range of block sizes. A model combining slow and fast varying errors into a total error Δ_a is used:

$$\Delta_a = a_0 + a_1 T_{\rm a} + a_2 T_{\rm a}^2 + \dots + a_n T_a^n + a_{\rm me} \sin(2\pi f_{\rm me} T_a),$$

where a_0 , a_1 , a_2 and a_n are the coefficients of the slow varying error polynomial, $f_{\rm me}$ is the frequency of the fast varying component of amplitude $a_{\rm me}$ and T_a is the aperture time . The frequency of Δ_a can be computed using [7]:

$$f_{me} = \frac{2}{\lambda} \frac{d\Delta_a}{dT_a}.$$
 (3)

The LOS error of any range bin can be used in (3) assuming the frequency of aperture-dependent motion error is range-invariant. A f_{me} larger than $1/T_a$ is considered as fast varying error [7]. The length of the aperture, which falls under the high frequency error region, is divided into smaller blocks and the remaining length is divided using larger blocks. As the focusing of different range bins are also determined by block sizes, the algorithm uses relatively larger blocks at far rather than near range.

The flowchart of the adaptive block-based SATA is given in Fig. 2. The time domain data, after performing coarse MOCO, are supplied to the adaptive SATA block. The sectioning of the aperture is performed using the slope information of the LOS deviation. The data are also divided into two sections in the range direction to allow range-dependent blocking. Smaller block size sets are used for ranges at or below reference and larger sets are reserved for far range. For perfect signal reconstruction, an overlap factor of 0.5 is used. One problem with adaptive SATA is that the sidelobe levels can become high due to the larger phase changes within unequal blocks (slow and fast error sections). One way to suppress the sidelobe levels is to zero pad the error sections to the full length both in aperture and range. This can smooth transition between blocks. The MOCO technique is similar to SATA [1] but with adaptive block and overlap sizes. Range cell migration correction (RCMC) and azimuth compression are performed on the corrected data to obtain the focused image.

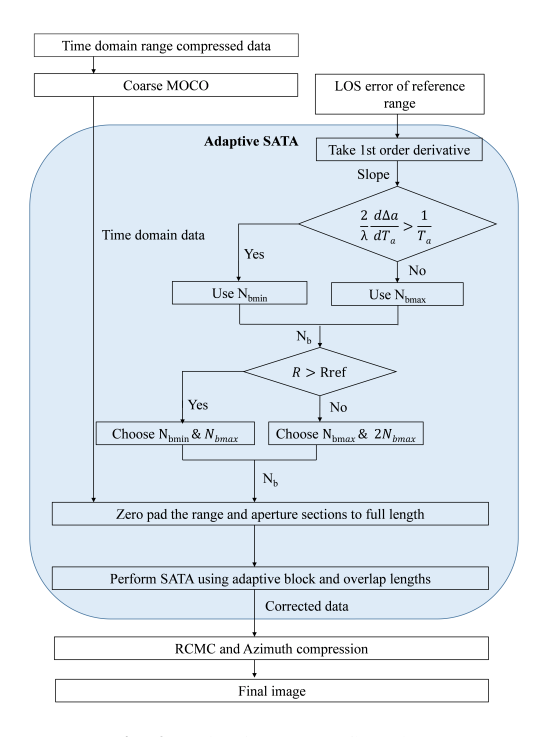


Fig. 2: Adaptive SATA flowchart

3.2. Apodization on SATA

Traditionally CDA is a technique to enhance the sidelobe levels of SAR images while preserving the mainlobe width [6]. It utilizes the complex impulse responses of a target generated using rectangular and Hanning windows and operates separately on the real and imaginary parts. For the real parts, at every spatial location, it compares the two values to find a sign change between them and uses a zero at that location if it detects a sign change. If the signs are the same, CDA chooses the absolute minimum of the two. The operation is repeated for the imaginary parts. As the sidelobes of the impulse responses have opposite signs, the lowest level of the two is obtained in CDA as a result.

Since CDA can optimize target responses based on different window functions, the concept can be well-suited to improve SATA where different block lengths are used. If the impulse responses of two targets focused using different blocks show sign changes, then according to CDA, there will be a block length in between where the response will be zero. It is possible that the optimal resolution and sidelobe of a target are obtained at two different blocks, then the minimization via CDA can be used to achiever better focusing.

4. EXPERIMENTAL RESULTS

Parameters	Simulated scenario	PLIS	
Centre frequency	1.26 GHz		
Range bandwidth	$30\mathrm{MHz}$		
Azimuth beamwidth	$25.5\deg$		
Aperture time	17.4 sec		
Nominal platform speed	$77\mathrm{m/s}$		
Scene centre	$3.011\mathrm{km}$		
PRF	285.714 Hz	$625\mathrm{Hz}$	
Platform height	$1850{\rm m}$	$1901.87\mathrm{m}$	
Swath width	$2.2\mathrm{km}$	$2.6\mathrm{km}$	

Table 1: SAR parameters

The performances of adaptive blocking and apodization based SATA are verified both with the simulated and real L-band datasets. The simulation parameters are tabulated in Table 1. Slow varying errors of up to cubic terms and fast-varying error being a combination of two sinusoids at 5 and 10 cycles per aperture and amplitudes 3 and 2 meters, respectively. The frequency of motion error is varied from slow to fast over the aperture. The maximum LOS deviation is 17 m.

Adaptive SATA is applied to the two targets described in Sec 2. To accommodate both $f_{\rm me}$ and $\theta_{\rm inst.}$, block sizes between 32 and 128 are used. A Hamming window is used to construct the PSFs. The simulation results for the targets are given in Table 2. For the scene-centre target, the ISLR level is particularly high with fixed block sizes. Adaptive SATA improved the ISLR by around 5 dB without affecting the resolution much. For the far range targets affected by smaller block sizes, the block length is increased beyond the reference. It results in a finer resolution of the target without any

Scene-centre	SATA		Adaptive SATA
	$N_b = 32$	$N_b = 64$	$32 \le N_b \le 64$
3dB width [m]	0.354	0.350	0.354
PSLR [dB]	-27.992	-28.897	-27.265
ISLR [dB]	-9.914	-13.247	-18.298
Far range	SATA		Adaptive SATA
	$N_b = 32$	$N_b = 128$	$32 \le N_b \le 128$
3dB width [m]	0.374	0.3745	0.347
PSLR [dB]	-11.13	-11.57	-11.08
ISLR [dB]	-8.91	-8.20	-8.29

Table 2: Near and far range target improvements in simulated scene with adaptive SATA.

notable increase in sidelobes. The results from apodization on the reference range target are shown in Table 3. As optimal resolution occurred at a different block length than that for an optimal sidelobe level for fixed block length SATA, application of apodization accumulated the optimal parameters.

	SATA		Apodized SATA
	$N_b = 64$	$N_b = 128$	
3dB width [m]	0.348	0.374	0.361
PSLR [dB]	-28.897	-29.683	-29.744
ISLR [dB]	-13.247	-16.254	-17.627

Table 3: Simulated target enhancement with apodization

Real data from an airborne polarimetric L-band imaging SAR (PLIS) are used with the proposed methods. Note that PLIS is high resolution SAR system with parameters shown in Table 1 [8]. The real data has a maximum LOS deviation of $20\,\mathrm{m}$ containing both low and high frequency errors. The high frequency component has up to 4 cycles per aperture time. A presumming operation is performed on the data, yielding an azimuth sample spacing of $0.5\,\mathrm{m}$. No weighting is applied in this case. Block sizes between 16 and 256 are used for adaptive SATA.

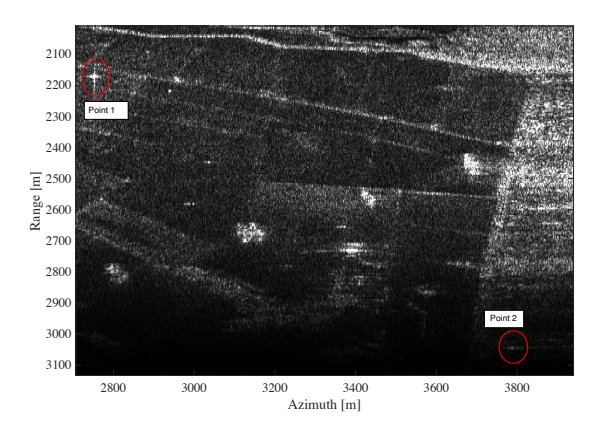


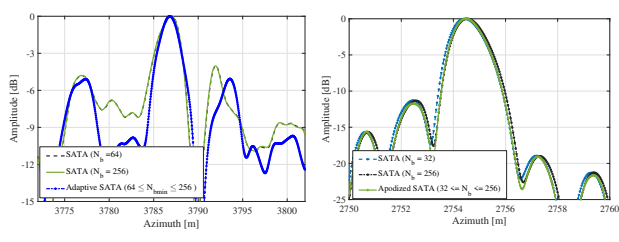
Fig. 3: PLIS image

The results for two point targets in Fig. 3, focused using conventional SATA with $N_b=64$, are discussed here. Points

1 and 2 are located at (down range) 2173 m and 3043 m, respectively. As in the simulated case, an increased ISLR suppression for near range point 1 is obtained in PLIS that is $1.38 \, dB$ lower than the lowest ISLR in SATA ($-8.61 \, dB$ at $N_b = 16$). However, a loss of resolution of less than a half the sample space (0.4 m) and PSLR level (4.88 dB) compared to conventional SATA are observed. This suggests further study is required to apply adaptive SATA to near range. The technique improves the far range (point 2) focusing in the real scenario, as shown in Fig. 4a and Table 4. The overall focusing quality of the target is improved via adaptive blocking, validating its usefulness for scenes where the swath width is large. One shortcoming of this technique is that it introduces a range-dependent azimuthal shift. The shift is due to combining aperture sections which are compensated for slightly different amounts of linear error computed by different block sizes. For far range targets, the shift can be more than half a resolution cell that will require relocation afterwards. Target PSFs, regardless of their position, can be sharpened using the apodization. Results for the near range point 1 before and after apodization are shown in Fig. 4b and Table 4. Both the resolution and PSLR are enhanced without impacting the ISLR much.

Far range	SATA		Adaptive SATA
	$N_b = 64$	$N_b = 256$	$64 \le N_b \le 256$
3dB width [m]	3.117	3.117	2.789
PSLR [dB]	-4.01	-4.02	-5.07
ISLR [dB]	-13.41	-13.34	-14.08
Near range	SATA		Apodized SATA
	$N_b = 32$	$N_b = 256$	
3dB width [m]	1.378	1.378	1.312
PSLR [dB]	-11.29	-11.34	-11.74
ISLR [dB]	-8.70	-8.73	-8.47

Table 4: PLIS target improvement with adaptive and apodized SATA



- (a) Far range, adaptive SATA
- (b) Near range, Apodized SATA

Fig. 4: PLIS focusing improvement

5. CONCLUSION

The high frequency motion error requires smaller blocks to be chosen while performing the aperture-dependent MOCO using SATA. Smaller blocks reduce its ability to accommodate finer squint angles within a block and increases the computational time. An analysis of the effects of subaperture blocks on the algorithm's performance is presented. Two techniques based on adaptive blocking and apodization are proposed to circumvent the aforementioned trade-off. The adaptive blocking scheme shows significant improvement in the overall focusing quality for far range targets. Target PSF enhancement can also be achieved by applying apodization irrespective of their range. Application of these techniques on real and simulated datasets confirm their applicability in both cases.

6. REFERENCES

- A. Potsis, A. Reigber, J. Mittermayer, A. Moreira, and N. Uzunoglou, "Sub-aperture algorithm for motion compensation improvement in wide-beam SAR data processing," *Electronics Letters*, vol. 37, no. 23, pp. 1405–1407, 2001.
- [2] K. A. C. de Macedo and R. Scheiber, "Precise topography- and aperture-dependent motion compensation for airborne SAR," *IEEE Geoscience and Remote Sensing Letters*, vol. 2, no. 2, pp. 172–176, 2005.
- [3] X. Zheng, W. Yu, and Z. Li, "A novel algorithm for wide beam SAR motion compensation based on frequency division," in 2006 IEEE International Symposium on Geoscience and Remote Sensing, 2006, pp. 3160–3163.
- [4] P. Pau, K. A. C. de Macedo, A. Reigbar, R. Scheiber, and J. J. Mallorqui, "Comparison of topography-and aperture-dependent motion compensation algorithms for airborne SAR," *IEEE Geoscience and Remote Sensing Letters*, vol. 4, pp. 349–353, July 2007.
- [5] L. Zhang, G. Wang, Z. Qiao, and H. Wang, "Azimuth motion compensation with improved subaperture algorithm for airborne SAR imaging," *IEEE Journal of Selected Topics in Applied Earth Observations and Remote Sensing*, vol. 10, no. 1, pp. 184–193, 2017.
- [6] H. C. Stankwitz, R. J. Dallaire, and J. R. Fienup, "Spatially variant apodization for sidelobe control in SAR imagery," in *Proceedings of 1994 IEEE National Radar Conference*, 1994, pp. 132–137.
- [7] W. G. Carrara, R. S. Goodman, and R. M. Majewski, Spotlight Synthetic Aperture Radar Signal Processing Algorithms, Artech House, Inc., Boston, 1995.
- [8] L. Zhu, J. P. Walker, N. Ye, C. Rüdiger, J. M. Hacker, R. Panciera, Mihai A. Tanase, X. Wu, D. A. Gray, N. Stacy, A. Goh, H. Yardley, and J. Mead, "The polarimetric L-Band imaging synthetic aperture radar (PLIS): Description, calibration, and cross-validation," *IEEE Journal of Selected Topics in Applied Earth Observations and Remote Sensing*, vol. 11, no. 11, pp. 4513–4525, 2018.